ELSEVIER

Contents lists available at ScienceDirect

International Journal of Pharmaceutics

journal homepage: www.elsevier.com/locate/ijpharm





Portable semisolid extrusion device for the production of personalized medicines in diverse settings

Paola Carou-Senra ^{a,1}, Lucía Rodríguez-Pombo ^{a,1}, Laura Castro-Martínez ^a, Abdul W. Basit ^{b,c,d,*}, Carmen Alvarez-Lorenzo ^{a,*}, Alvaro Goyanes ^{a,b,c,d}

- ^a Departamento de Farmacología, Farmacia y Tecnología Farmacéutica, I+D Farma (GI-1645), Facultad de Farmacia, Instituto de Materiales (iMATUS) and Health Research Institute of Santiago de Compostela (IDIS), Universidade de Santiago de Compostela 15782 Santiago de Compostela, Spain
- b Department of Pharmaceutics, UCL School of Pharmacy, University College London, 29-39 Brunswick Square, London WC1N 1AX, UK
- ^c FABRX Ltd., Henwood House, Henwood, Ashford, Kent TN24 8DH, UK
- ^d FABRX Artificial Intelligence, Enrique Vidal Abascal 7, Santiago de Compostela, CP 15702, Spain

ARTICLE INFO

Keywords: Personalized medications Rare diseases Decentralised on-demand production Pen printing of pharmaceuticals Handheld devices Additive manufacturing

ABSTRACT

The potential of 3D printing (3DP) in personalized medicine has led to the development of various pharmaceutical-grade printers, advancing its integration into clinical practice. However, accessible and decentralized solutions are still required to enable on-demand drug production in remote or resource-limited settings. Handheld 3D pens offer a compact, portable, and energy-efficient alternative, particularly suited for small pharmacies, mobile clinics, emergency operations, and underserved regions. This study presents the first application of a handheld 3D pen using semisolid extrusion (SSE) technology for the precise fabrication of citrulline lozenges (200-700 mg). Citrulline, an amino acid used in the treatment of rare diseases, was formulated into two pharma-ink bars containing 30 % and 50 % w/w citrulline. Minimal materials were used, with isomalt, a sugar substitute, as the main excipient along with water, and no organic solvents were involved. Dose personalization was evaluated by selecting the printed area and the printing time, with a strong correlation observed between printing time and final dose. The printed lozenges exhibited excellent dose accuracy and recovery (~100 %), while dissolution tests reported an 80 % of citrulline released within the first 12 min. The pharma-ink bars remained stable over one month, exhibiting minimal water loss (~2%) and retaining both printability and drug integrity. These findings establish handheld 3D pens as environmentally-friendly technology for rapid personalized drug manufacturing. The combination of stable pharma-inks and precise dose control underscores its potential for decentralized, on-demand production of personalized therapies in remote and resource-constrained environments.

1. Introduction

In recent years, 3D printing (3DP) technologies have been explored in the pharmaceutical field as tools that help to automate the manufacturing of small batches of personalized medicines (Ehtezazi et al., 2018; Milliken et al., 2024; Tong et al., 2024). The immense potential of pharmaceutical 3D printing has driven its rapid adoption and evolution. While early applications relied on commercial printers designed for other purposes (Genina et al., 2013; Kumari et al., 2024), the outstanding results soon highlighted the need for more tailored

solutions. This led to the development of specialized hardware and software for the 3D printing of pharmaceuticals. In response, a new generation of pharmaceutical grade 3D printers has emerged (Ianno et al., 2024) helping to bring printing technologies closer to real-world therapeutic scenarios (Rodríguez-Pombo et al., 2024).

While these pharmaceutical printers offer remarkable versatility, their size and infrastructure requirements often limit their use in centralized facilities, such as research laboratories or hospitals without dedicated printing spaces. In contrast, portable printing devices present a compelling alternative, offering unique advantages that could

^{*} Corresponding authors at: Department of Pharmaceutics, UCL School of Pharmacy, University College London, 29-39 Brunswick Square, London WC1N 1AX, UK (A. W. Basit).

E-mail addresses: a.basit@ucl.ac.uk (A.W. Basit), carmen.alvarez.lorenzo@usc.es (C. Alvarez-Lorenzo).

¹ These authors contributed equally to this work.

significantly expand the reach of on-demand manufacturing.

Handheld printers could provide several benefits over desktop printers, becoming a practical choice in many scenarios. Their compact size allows for significant space savings, making these devices ideal for places with limited room. Unlike large printers that require a constant power supply and consume more energy, handheld printers are more energy-efficient—they can stay connected while using less power, operate unplugged after charging, or be powered by alternative sources like batteries. Moreover, their portability enables easy transportation and use in diverse settings. As a result, handheld printers could be particularly useful in environments where other printers would be impractical, such as small community pharmacies (e.g. rural pharmacies), underdeveloped locations with limited infrastructure, emergency response situations, military camps, and mobile healthcare units. In this way, handheld printers could bring on-demand production of personalized medicines closer to previously inaccessible spaces, offering a costeffective and resource-efficiency optimized alternative while saving energy and space, and ensuring easy portability.

In fact, the concept of portable printing devices has already been explored in other techniques, such as inkjet printing. A handheld printer was successfully implemented for the rapid production of buccal films containing flexible and precise doses of nicotine (ranging from 0.60 to 4.30 mg) (Carou-Senra et al., 2025). The portable inkjet printing device did not only allow the rapid adaption of gradual therapies, but also the production of individualized treatments within seconds. Later, a handheld inkjet printer was also used for tattoo printing of a hormone, oestradiol, for replacement therapy (Januskaite et al., 2025). This advancement demonstrated in inkjet printing could be extrapolated to other 3DP technologies.

One of the most widely used and even clinically implemented techniques is Semisolid Extrusion (SSE) (Rodríguez-Pombo et al., 2024a,b; Liu et al., 2023). SSE is a material extrusion technique that builds 3D objects by depositing gels or pastes in sequential layers (Lyousoufi et al., 2023). Using semi-solid extrusion, it has been possible to develop novel pharmaceutical dosage forms that allow greater personalization of treatments, such as polypills (Khaled et al., 2015), tablets (Cui et al. 2020), chewable formulations (Karavasili et al. 2020), or orodispersible films (ODFs) (Sjöholm and Sandler, 2019). Following the principle of implementing new portable devices, adapting a handheld system specifically for SSE would represent a significant step forward. Such development could bring this well-established technology closer to less accessible environments, extending its reach beyond traditional manufacturing settings and enhancing its adaptability for decentralized production of personalized medicines.

3D pens are emerging as innovative devices that bring the capabilities of 3DP technologies to a portable format, allowing users to easily draw and create their own objects (Seoane-Viaño et al., 2021). Some of these pens focus on filament extrusion, enabling the creation of various 3D structures, while others extrude bars, producing edible objects such as candies. The latter can be closely compared to SSE, where a gel or paste is extruded by a plunger through a nozzle applying temperature. By replacing commercial bars with pharma-ink bars, this concept could be adapted to produce medicated lozenges; namely, a type of hard candy-like dosage form designed to be dissolved in the mouth rather than swallowed. We hypothesize that the formulation of these pharmaink bars can be adapted not only to different doses or pharmacokinetic requirements but also to patient preferences regarding flavouring or colouring, enhancing their acceptance using minimal material and energy resources. This alternative pharmaceutical form is particularly beneficial for certain populations, such as paediatrics, elderly, or individuals with swallowing difficulties. Moreover, due to their mechanism of dissolving in the mouth, lozenges can be used for both systemic and local treatments.

The aim of this study was to adapt and implement, for the first time, a 3D pen (Polaroid Candy 3D Pen) for the production of small batches of 3D printed personalized lozenges (printlets). Citrulline, a dietetic

product employed for the treatment of a paediatric rare disease (ornithine transcarbamylase deficiency, OTC Deficiency), was used as a model compound to prepare the pharma-inks bars with tailored doses. For this purpose, various pharma-inks bars containing different loadings of citrulline (30 and 50 % w/w) were prepared and extensively characterized. Isomalt, a sugar-substitute, was used as a main excipient, and no-organic solvents were involved in bars production. Two different printing parameters (area and time) were evaluated to obtain personalized doses. Citrulline content of printlets along with its dissolution behaviour was fully studied. Moreover, the physicochemical properties of these printlets and pharma-ink bars were also investigated. Lastly, stability tests were carried out in the pharma-ink bars after 30-day storage period to evaluate its printability as well as the potential citrulline degradation over time.

2. Materials and Methods

2.1. Materials

Isomalt Galen IQTM 960 (Mw = 344.3 g/mol) was from BENEO-Palatinit GmbH (Mannheim, Germany); L-citrulline (CIT) (Mw = 175.2 g/mol) was from Medical Nutrition (Cantabria Labs, Madrid, Spain); the red food dye for pink colour was purchased from Acofarma (Barcelona, Spain) and the blue food dye from Guinama (Valencia, Spain). Strawberry and banana flavourings were from Acofarma (Barcelona, Spain). Simulated saliva (pH = 6.75 \pm 0.05) was prepared dissolving 2.38 g Na₂HPO₄ (Scharlab S.L; Barcelona, Spain), 0.19 g KH₂PO₄ (ITW Reagents; Darmstadt, Germany) and 8.00 g NaCl (Scharlab S.L.; Barcelona, Spain) in MilliO water (Millipore, Madrid, Spain).

2.2. Preparation of pharma-ink bars

2.2.1. Elaboration process

Two different pharma-inks based on Isomalt Galen IQTM 960 were prepared containing 30 % w/w and 50 % w/w of citrulline, respectively (Table 1). Initially, isomalt (15 g) was weighed and transferred to a metal container, along with water (4 mL). The mixture was heated on a hot plate (MS-H280-Pro model) to 100 $^{\circ}$ C and stirred mechanically at 170 rpm (HEI-TORQUE 200, Heidolph Instruments, Schwabach, Germany) for 5 min. Once a homogeneous mixture was obtained, the temperature was reduced to 70 °C for the addition of the corresponding amount of citrulline under stirring and to prevent decomposition of the formulation. Colourant (200 µL) and flavouring (200 µL) were also added. Finally, the formulations were transferred to moulds previously designed to obtain bars with the appropriate shape and size for insertion into the printing device. The moulds were fabricated with specific sizes for the preparation of pharmaceutical bars with dimensions similar to those of the commercial bars used in the Candy Play 3D Pen (Fig. 1). The moulds were manufactured using a Fused Deposition Modeling (FDM) 3D printer (ILC V3 PREMIUM, 3D LimitLess, A Coruña, Spain) with a PLA filament spool. The molds were manufactured by FDM 3D printing (ILC V3 PREMIUM, 3D LimitLess) with a 750g PLA 1.75 mm filament spool. Tinkercad (Autodesk, Inc), a free and easy-to-use web application for 3D design, was used to design the parts. PrusaSlicer 2.8.0 (Prusa Research a.s.) was used as a slicer, an open-source tool that allows exporting the print files for the 3D printer.

Post-elaboration steps included the solidification of the pharma-ink

Pharma-inks developed with different contents in citrulline, colourant and flavouring.

Pharma-ink bar code	Citrulline (% w/w)	Colourant	Flavouring
CIT-30	30	Red	Strawberry
CIT-50	50	Blue	Banana



Fig. 1. Image of moulds with specified dimensions for producing pharmaceutical bars.

in the moulds, as explained below.

2.2.2. Conditions for solidification

To ensure proper solidification of the pharma-ink bars, three different storage conditions were evaluated at: (a) room temperature (~20 °C) in an oven (Heraeus I42, Hanau, Germany) as the most practical and representative environment for routine preparation; (b) 37 °C to simulate an accelerated storage condition; and (c) 4 °C to assess the impact of refrigeration. Each of these procedures was maintained for a period of 10 h. After this time, the bars were carefully unmoulded, avoiding any damage or breakage.

The weight loss due to water evaporation during the solidification stage was monitored for the moulds stored at 20 $^{\circ}$ C, from the time of filling to their subsequent removal 10 h later. To evaluate whether there were statistically significant differences in the water loss between moulds of both formulations (CIT-50 vs CIT-30), the normality of the data was first assessed using the Shapiro-Wilk test. The difference in variances was evaluated using the F-test. Finally, both formulations were compared using the Students t-test (p < 0.05).

2.3. Pharma-ink bars weight variation inter-batch and between formulations

The weight of the demoulded bars from both formulations (CIT-50 and CIT-30) was recorded using a ABT 220-4NM analytical balance (KERN & SOHN GmbH, Stuttgart, Germany). For this purpose, two bars were randomly selected and weighed from three different batches, resulting in a total of six measurements (n = 6) for each pharma-ink formulation. Inter-batch variability was evaluated using the Kruskal-Wallis test to compare batches within each formulation (p < 0.05). To determine whether there were statistically significant differences between the weights of CIT-50 and CIT-30, the normality of the data was first assessed using the Shapiro-Wilk test. Once normality was confirmed, the difference in variances was evaluated using the F-test. Finally, both formulations were compared using the Student's t-test (p < 0.05).

2.4. Pharma-ink bar water loss

Additionally, to assess water loss over time, pharma-ink bars (n = 6)

were stored under controlled conditions (20 $^{\circ}$ C in an oven), and their weights were recorded after 30-day using a ABT 220-4NM analytical balance (KERN & SOHN GmbH, Stuttgart, Germany). The percentage of weight loss was calculated using Equation (1):

Weight loss (%) =
$$\frac{\textit{Weight day 1 (g)} - \textit{Weight after } 30 - \textit{day (g)}}{\textit{Weight day 1 (g)}} x 100 \tag{1}$$

To evaluate statistical differences in water loss variability, inter-batch variability was analysed separately for each formulation using the Kruskal-Wallis test, comparing batches within CIT-50 and CIT-30 independently (p < 0.05). Finally, to determine whether water loss differed between CIT-50 vs CIT-30, normality was assessed using Shapiro-Wilk test and difference in variances was evaluated using F-test. Finally, both formulations were compared using Student's t-test (p < 0.05).

2.5. Pharma-ink bars fracture toughness

After demoulding, the fracture toughness of the CIT-50 and CIT-30 pharma-ink bars was evaluated using a Type 1B 24 Durometer (Erweka-Apparatus, Heusenstamm, Germany). Commercial bars were also assessed for comparison. Additionally, the fracture toughness of pharma-ink bars was evaluated after a 30-day storage period under controlled conditions to analyse possible changes overtime.

Bars were carefully placed horizontally and aligned in the device's holder to ensure even application of force across their surface (Fig. 2). The durometer was positioned perpendicular to the surface of the bars, ensuring that the indenter was in contact with the bar. Force was applied from the indenter into the bars, and the resulting fracture toughness value was displayed on a scale from 0 to 150 N. All tests were performed in duplicate (n = 2), and results were expressed as mean \pm standard deviation (SD).

A statistical analysis was performed to evaluate whether there were



Fig. 2. Image of CIT-30 pharma ink bar positioned on the durometer for performing the fracture toughness test.

significant differences in fracture toughness between immediately demoulded pharma-ink bars of both formulations (CIT-50 vs CIT-30) using the Mann-Whitney U test (p < 0.05). Additionally, the Mann-Whitney U test was also used to assess whether there were statistically significant differences in fracture toughness within the same formulation, comparing bars measured immediately after demoulding and after 30-day of storage (fresh bars vs 30-day storage bars), with a significance threshold of p < 0.05.

2.6. 3D printing process

Citrulline printlets were obtained using the Candy Play 3D Pen printer (Polaroid, Minnetonka, MN, USA) (Fig. 3A). The different parts of 3D pen and the printing process are illustrated in Fig. 3B. The bars were inserted into the 3D pen's loading point. Once inside, the activation button was pressed, causing the plunger to descend and slide the bars toward the thermal resistor. The temperature of $100\,^{\circ}\text{C}$ caused the bar to melt, and the plunger extruded the ink through the nozzle (0.80 mm inner diameter), enabling the creation of various figures.

To avoid cross-contamination and microbiological risks, after each printing process with both CIT-30 and CIT-50 formulations, the pen was disassembled. The parts that were in direct contact with the formulation were then cleaned following a standardized procedure: first washed with water at $100\,^{\circ}\text{C}$ for 30 min, followed by rinsing with ethanol, and finally with distilled water.

To print personalized doses, two key parameters were tested: area (cm^2) and printing time. For area testing, different dimensions in width x length (2 x 1, 2 x 2 and 2 x 4 cm) were manually design and print. While for time testing, cylindrical shapes were manually drawn with different printing times 30 s, 45 s and 60 s. After printing process, all the printlets were stored in Class B X-Large amber PVC blisters (Health Care Logistics, Circleville, USA) for later evaluation. For the following experiments, printlets obtained at different printing times were used.

2.7. Pharma-ink bars and printlet characterization

2.7.1. X-ray powder diffraction (XRPD)

To evaluate the crystallinity index, pure isomalt, pure citrulline, CIT-30 and CIT-50 pharma-inks bars and printlets were analysed by X-ray diffraction. The X-ray powder diffraction (XRPD) data were collected using Göebel geometry with parallel beams on a Bruker D8 Advance (Bruker Corporation, Billerica, MA, USA) X-ray diffractometer (40 kV, 40 mA, theta/theta) equipped with a sealed Cu X-ray tube (CuKα1, $\lambda=1.5406~\text{Å})$ and a LYNXEYE-2 detector. Diffractograms were obtained in the angular range of 3 to $40^{\circ}~2\theta$ with a step size of 0.02° and a counting time of 2 s per step.

Samples were deposited on an oriented crystal substrate (Si 511 plate) to minimize background scattering caused by glass-type supports. Mathematical analysis of the obtained diffractograms was performed using the software HighScore Plus, Version 3.0d (Malvern Panalytica, Grovewood Road, UK).

2.7.2. Differential Scanning Calorimetry (DSC)

DSC scans of pure isomalt, pure citrulline, CIT-30 and CIT-50 pharma-inks bars and printlets were recorded at a heating rate of 10 °C/min in a DSC Q100 (TA Instruments, New Castle, DE, USA) fitted with a refrigerated cooling accessory. The temperature range was 40–350 °C and nitrogen was used as the purge gas (50 mL/min). All experiments were performed using non-hermetic aluminium pans, in which 2–4 mg of sample was accurately weighed using the precision balance (0.0001 mg) of TGA55 Discovery series equipment (TA Instruments, New Castle, DE, USA). Data were collected with the TA Advantage software for Q series (version 2.8) and analysed using TA Instruments Universal Analysis 2000 (version 4.5.0.5).

2.7.3. Fourier-transform infrared spectroscopy (FTIR)

FTIR spectra of pure isomalt, pure citrulline, CIT-30 and CIT-50 pharma-inks and printlets were collected using a Spectrum 100 FTIR spectrometer (PerkinElmer, Waltham, MA). All samples were scanned between 4000 and 400 $\,{\rm cm}^{-1}$ at a resolution of 1 $\,{\rm cm}^{-1}$ resolution for 6 scans

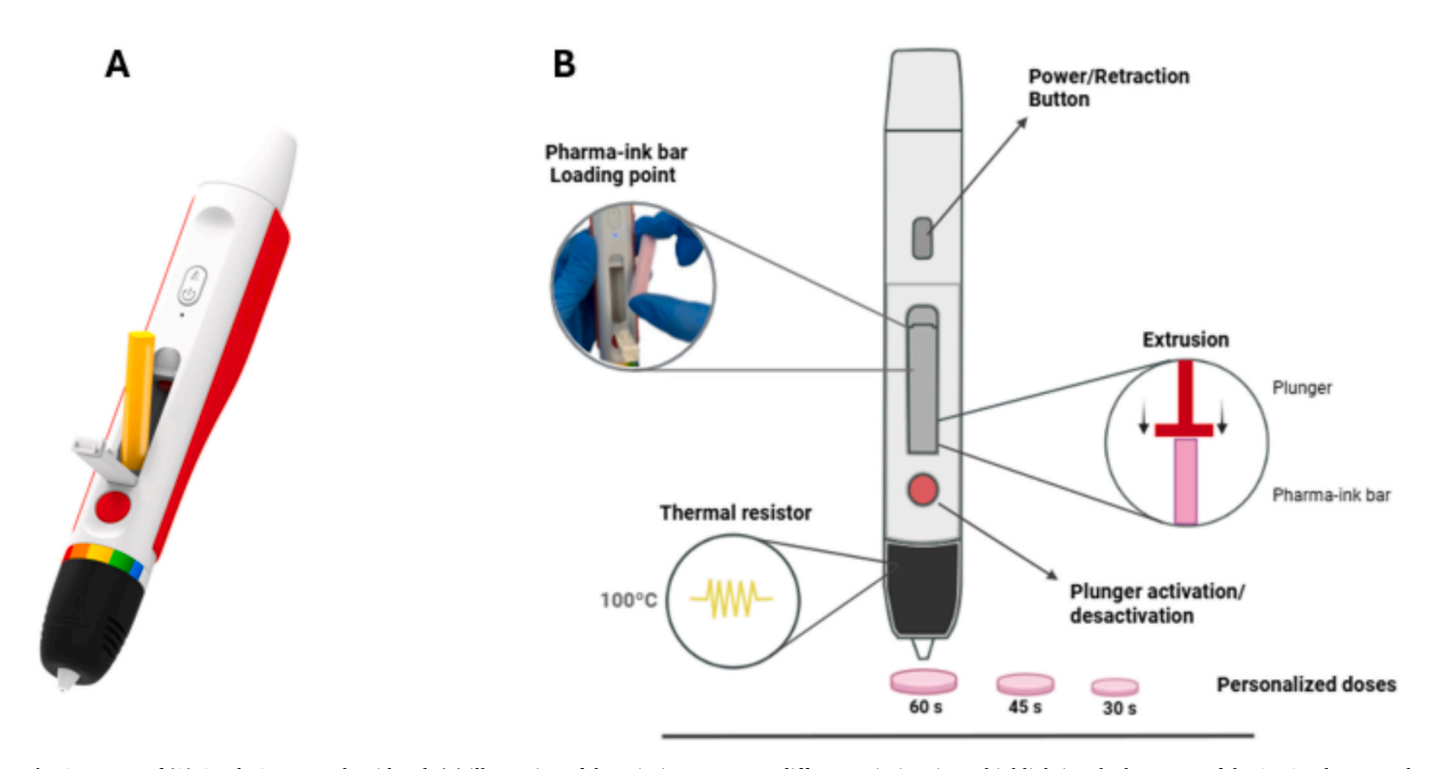


Fig. 3. Image of (A) Candy 3D pen Polaroid and, (B) illustration of the printing process at different printing times, highlighting the key parts of the 3D Candy Pen and main steps involved in the printlets production.

2.8. Weight variation of printlets

5 Printlets from of each pharma-ink (CIT-30 and CIT-50) and printing time (30 s, 45 s and 60 s) were individually weighed using an analytical balance (KERN PEJ model, KERN & SOHN, Balinge, Germany). The data were reported as the mean weight \pm SD (n = 5), and the coefficient of variation (CV) was calculated as Equation (2)

$$CV(\%) = \frac{SD}{Mean\ weigh} x 100 \tag{2}$$

2.9. Citrulline content in printlets

Printlets of each pharma-ink and different printing times were placed individually in 100 mL of Milli-Q® water and left to dissolve under magnetic stirring (250 rpm) until complete extraction of citrulline (approx. 1 h). Aliquots of solutions were filtered through 0.22 µm polytetrafluoroethylene membrane (PTFE) hydrophilic filters (Millipore Ltd., Dublin, Ireland). The amino acid concentration was determined using high performance liquid chromatography-ultraviolet (HPLC-UV) (Agilent Technologies, Santa Clara, CA, USA). The assay involved injection of 20 μL samples using a mobile phase of 0.03 mM phosphoric acid through a Waters Spherisorb 3 µm ODS2 column, 4.6 mm x 150 mm column (Waters, Milford, MA, USA) maintained at 25 °C. The mobile phase was pumped at a flow rate of 0.7 mL/min and the eluent was analysed at 207 nm. All measurements were performed for the formulation with the minimum citrulline content (CIT-30) and the formulation with the maximum content (CIT-50) at three different printing times of 30, 45 and 60 s. The retention time was 2.67 min, and the concentration range was 2 to 210 $\mu g/mL$. The data were reported as the mean dose \pm SD (n = 5).

Recovery was calculated to determine the actual amount of drug in each printlet, based on its mass and the known concentration of amino acid in the pharma-ink. This value was compared to the theoretical dose expected from the printlet's weight and formulation. Recovery was calculated as Equation (3):

Recovery (%) =
$$\frac{Experimental\ dose\ (mg)}{Theoretical\ dose\ (mg)}x100 \tag{3}$$

Dose accuracy was referred to the estimated dose expected for a specific formulation and printing time. It was calculated in reference to the dose obtained for printlets prepared with a longer printing time (60 s) for each formulation, considering them as the reference value, e.g. for 30 s it was expected to obtain half of the dose obtained from 60 s printlets. Dose Accuracy was calculated as Equation (4):

Dose accuracy (%) =
$$\frac{Experimental\ dose\ (mg)}{Theoretical\ dose\ (mg)}x100$$
 (4)

2.10. In vitro disintegration test

The disintegration test of CIT-30 and CIT-50 printlets obtained at lower (30 s) and higher (60 s) printing time (mean weight in Table 2) was performed, in triplicate, using a disintegration apparatus consisting

of a basket-rack assembly which complies with European Pharmacopoeia (European Pharmacopoeia, 2025a). The test was conducted using 700 mL of simulated saliva (pH $=6.8\pm0.5$) to mimic the fluid of the oral cavity. The temperature of the external bath was set in 37 \pm 0.5 °C. Samples were subjected to a constant shaken of 30 cycles per minute. Plastic discs were used to prevent floating of the samples. After 15 min, the basket assembly was removed from the apparatus, and the state of each printlet was evaluated (n = 3). According to the European Pharmacopoeia, complete disintegration is defined as that state in which any residue of the unit, except fragments of insoluble coating or capsule shell, remaining on the screen of the test apparatus or adhering to the lower surface of the discs, if used, is a soft mass having no palpably firm core.

The average disintegration rate was calculated for each formulation and printing time. This method was applied to reduce the influence of individual printlet mass variability, normalizing the disintegration data and, also, focusing the analysis on the intrinsic properties of each formulation. Average disintegration time was calculated as Equation (5):

Average disintegration rate
$$\left[\frac{mg}{s}\right] = \frac{printlet\ mass\ [mg]}{Disintegration\ time\ [s]}$$
 (5)

2.11. In vitro dissolution test

Citrulline release profiles were evaluated using a VWR® Advanced Mini Shaker (VWR Advanced Mini Shaker; VWR, Radnor, PA, USA). The stirring speed was set at 100 rpm with a temperature of $37\pm0.5\,^{\circ}\text{C}$. The dissolution medium used was 50 mL of simulated saliva (pH = 6.8) to mimic physiological conditions. At 2 min time intervals, samples of 2 mL were removed and replaced with fresh prewarmed medium to maintain sink conditions. Aliquots were filtered through 0.22 μm hydrophilic filters (Millipore Ltd., Ireland) and analysed using the HPLC method (described in Section 2.9) to determine the amount of citrulline released at each time. The test was extended to 45 min to ensure complete dissolution. All measurements were performed in triplicate for CIT-30 and CIT-50 printlets obtained at lower (30 s) and higher (60 s) printing time (mean printlets weight and citrulline contents are compiled in Table 2). Data were reported as mean \pm SD (n = 3).

2.12. Stability assessment of pharma-ink bars

To assess the stability of citrulline in the pharma-ink bars and to detect any potential amino acid degradation, pharma-ink bars of CIT-30 and CIT-50 were stored in zip bags for 30-day at 20 $^{\circ}$ C in an oven (Heraeus I42, Hanau, Germany). After 30-day storage period, the pharma-ink bars were printed for 30 s (the lowest printing time) and 60 s (the highest printing time). Citrulline content, recovery and dose accuracy were calculated as reported in Section 2.9. Recovery informed about potential citrulline degradation over time. Dose accuracy was calculated to check whether the same amount of citrulline (at 30 s and 60 s) was correctly deposited after 30-day of storage regarding flowability. The doses obtained from the printlets produced within 60 s using fresh bars were used as a reference for each formulation to calculate the

Table 2 Dose and weight of printlets produced using CIT-30 and CIT-50 pharma-inks at different printing times, coefficient of variation (CV), dose accuracy and recovery. Results are shown as mean \pm SD (n = 5).

Formulation code	Printing time (s)	Dose (mg)	Weight (mg)	CV (%)	Dose accuracy (%)	Recovery (%)
CIT-30-30	30	204.8 ± 4.3	679.6 ± 5.7	0.84	101.90 ± 0.85	100.45 ± 1.64
CIT-30-45	45	300.2 ± 7.2	1007.0 ± 23.3	2.32	100.66 ± 2.33	99.36 ± 1.50
CIT-30-60	60	402.3 ± 14.7	1349.6 ± 43.5	3.23		99.38 ± 2.16
CIT-50-30	30	354.9 ± 8.2	715.7 ± 21.2	2.96	99.64 ± 2.95	99.19 ± 1.30
CIT-50-45	45	535.1 ± 3.6	1079.0 ± 21.0	1.94	100.22 ± 1.95	99.81 ± 0.57
CIT-50-60	60	718.2 ± 5.2	1444.9 ± 10.2	0.71		99.50 ± 0.61

dose accuracy. In this way, the dose obtained, for example, with the stored bars of CIT-30–60 s after 30-days should be similar to that obtained with the fresh bars if there were a consistent deposition of pharma-ink. Data were reported as mean \pm SD (n = 5).

A statistical analysis was performed to assess differences in recovery for each formulation, comparing recovery of printlets obtained from fresh bars and from those stored after 30-days. First, the Shapiro-Wilk test was applied to determine whether the data followed a normal distribution. If normality was confirmed, variance homogeneity was assessed using the F-test. For the comparison of recovery between printlets obtained from fresh and stored bars within each formulation code (CIT-30–30, CIT-30–60, CIT-50–30, CIT-50–60), a Student's *t*-test was conducted (p-value < 0.05).

2.13. Statistical analysis

All statistical analyses were conducted using GraphPad (GraphPad Prism 2019, GraphPad Software, Inc, CA, USA).

3. Results and Discussion

For the first time, a 3D Pen was adapted and used in the pharmaceutical field for the rapid and decentralised production of lozenges containing flexible and precise drug doses. Specifically, formulations containing 30 % w/w (CIT-30) and 50 % w/w (CIT-50) of citrulline were successfully developed. Isomalt, a polyol used as sugar substitute, was the main excipient. It offers several nutritional benefits such as a low glycaemic index and low insulinemic response, making it particularly suitable for children and people with diabetes. Additionally, isomalt is a tooth friendly excipient (preventing caries) and provides a low digestibility and low physiological energy value (approximately 8.4 kJ/g), further enhancing its suitability for health-conscious formulations (Schweitzer et al., 2024). Moreover, no organic-solvents were included in pharma-ink preparation.

3.1. Preparation of pharma-ink bars and printlets

The 3DP process first involved transferring the CIT-30 and CIT-50 pharma-inks into moulds (previously designed) to obtain pharma-ink bars. After solidification, these bars were inserted into the 3D Pen where they were heated at 100 °C and extruded, producing a range of artistic shapes— everything from whimsical dinosaurs to futuristic spaceships (Fig. 4). Such design flexibility may enhance the visual appeal of the pharmaceutical forms, and the incorporation of colouring and flavouring agents into the pharma-inks could further improve palatability and patient acceptability and adherence to the treatment

(Rodríguez-Pombo et al., 2024a). However, in a handheld system the appearance of complex geometries depends largely on the operator's dexterity, which limits rigorous morphological characterization. For this reason, the primary aim of the study was not to achieve geometric fidelity but to demonstrate a practical, resource-conscious approach in which printing time consistently correlated with reproducible weight and precise dosing of citrulline. Accordingly, cylindrical shapes—common in marketed medicines and well suited for reproducible testing—were adopted for most experiments.

A key factor in achieving these successful outcomes was the proper solidification of the pharma-inks withing the moulds. The optimal solidification condition was established at 20 $^{\circ}$ C in a controlled oven environment (Fig. 5A), guaranteeing consistency and integrity of the bars. The temperature of 37 $^{\circ}$ C caused cracks due to rapid water evaporation (Fig. 5B) while 4 $^{\circ}$ C resulted in soft bar that did not solidify properly (Fig. 5C).

Water loss during solidification stage in the moulds was evaluated for moulds stored at 20 °C. After 10 h, moulds containing CIT-50 pharmaink lost about a 0.14 \pm 0.05 % w/w of water, while CIT-30 moulds exhibited a water loss of 0.08 \pm 0.08 % w/w. No significant differences in water loss during solidification when comparing both formulations were found.

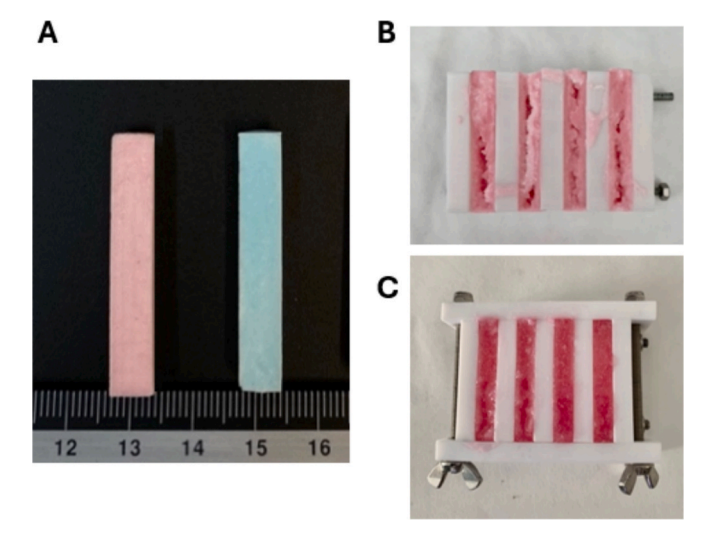


Fig. 5. Picture of moulds with CIT-30 (pink) and CIT-50 (blue) pharma-ink stored at: (A) 20° C in an oven, (B) 37° C in an oven and (C) at 4° C in a refrigerator. The scale bar indicates length in centimetres (cm).

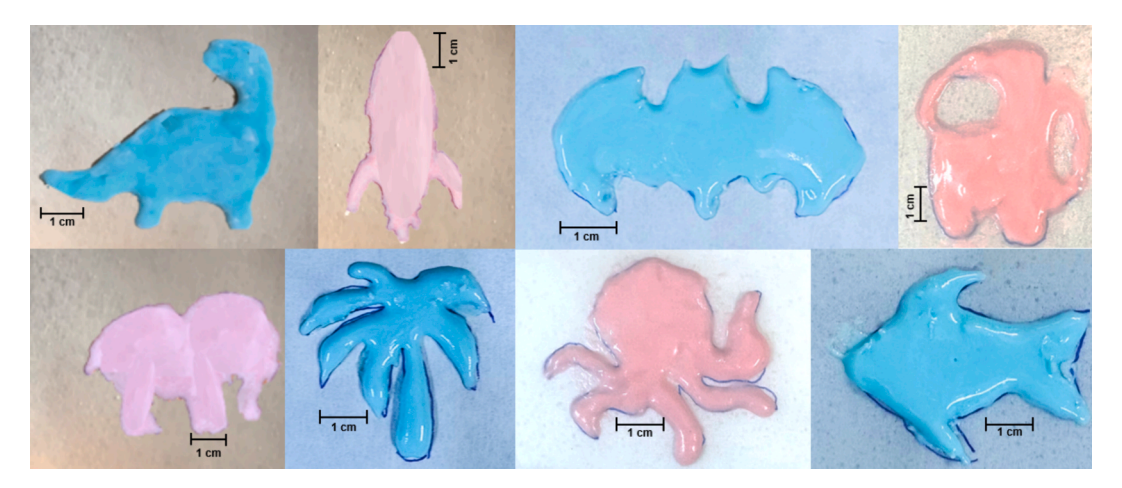


Fig. 4. Image of creative figures printed in the study using both pharma-inks from left-to-right from top-to-bottom: dinosaur; starship; batman icon; among us icon; elephant; palm tree; octopus and fish.

For more detailed characterization, pharma-ink bars from different batches were weighed (Fig. 6). CIT-50 pharma-ink bars had an average weight of 1.97 ± 0.02 g, while CIT-30 bars were slightly heavier, with an average weight of 2.22 ± 0.04 g. This higher weight in the CIT-30 bars could be attributed to the lower viscosity of CIT-30 formulation, which allowed better distribution throughout the mould, and consequently, more effective space filling. Since the printing temperature (100 $^{\circ}\text{C}$) exceeded the operating range of the available rheometers, viscosity could not be quantified; however, the lower resistance to flow was visually evident. Statistical tests revealed no significant differences in weight within batches of the same formulation. In contrast, a significant difference was observed when comparing CIT-30 and CIT-50 bars.

Additionally, pharma-ink bars were stored and weighed after 30 days to evaluate water loss during storage. CIT-50 pharma-ink bars lost an average of 2.41 \pm 0.62 % of their weight, while CIT-30 pharma-ink bars lost approximately 1.88 \pm 0.67 %. No significant differences in water loss between batches of the same formulation were found. Furthermore, the percentage of water loss did not vary significantly when comparing both CIT-30 vs CIT-50 bars, demonstrating a consistent water loss regardless of the pharma-ink formulation.

The fracture toughness of the pharma-ink bars was also studied and compared with commercial bars (Fig. 7). The CIT-50 pharma-ink bars exhibited slightly higher mean fracture toughness than CIT-30 pharma-ink bars, which could be attributed to the higher percentage of citrulline in their formulation that resulted in a denser structure. However, no statistically significant differences were found when comparing both formulations.

The commercial bars showed higher fracture toughness than the developed pharma-ink bars. The composition of the commercial bars consisted mainly of isomalt and aspartame (stated in the label). The absence of any pharmaceutical ingredient allowed the isomalt to form a more rigid structure. The possible interaction between isomalt and citrulline could disrupt isomalt crystalline structure, resulting in a softer texture.

Fracture toughness was also evaluated on pharma-ink bars stored for 30 days. Pharma-ink bars after 30 days exhibited slightly higher mean values (Fig. 7), but statistical analysis concluded that there were no significant differences in the fracture toughness of fresh bars and those stored for 30 days.

3.2. Printlets characterization

Dosing precision for personalized treatments was assessed in terms of two printing parameters: area (cm²) and time (s). The printed area was discarded due to the significant variability observed. A simple rectangle with 2×4 cm dimensions was initially designed for the evaluation. It was quickly demonstrated the low reproducibility achieved, since the printlet weight varied considerably, not only between different users but

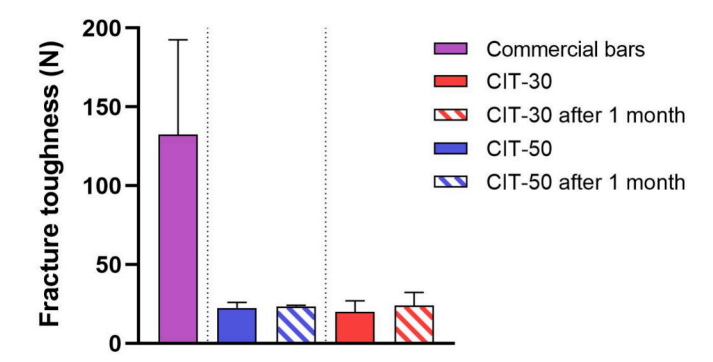


Fig. 7. Fracture toughness exhibited by commercial bars and CIT-30 and CIT-50 pharma-ink bars developed in the study.

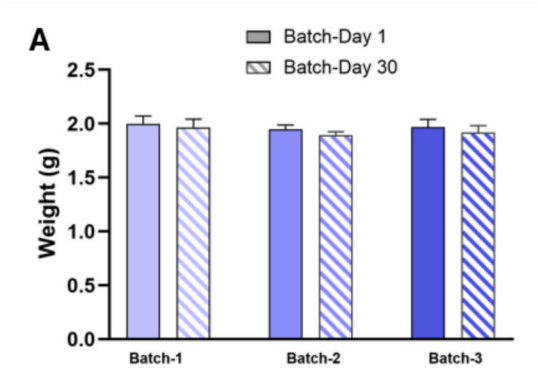
also for the same user within different replicates. This variability was primarily related to the printing speed and the pattern followed, both of which could greatly alter the amount of pharma-ink deposited for each printlet. Since this is a manual printing process, these last parameters could not be controlled so the use of the printed area to establish a relationship between dose and area was discarded.

Regarding the evaluation of the printing time, simple figures (cylinders) were printed for different preestablished times (30 s, 45 s and 60 s) in order to determine a relationship between the printing time and the dose (Fig. 8).

The results obtained showed good reproducibility (Table 2). The doses obtained ranged from 194 mg to 720 mg increasing logically with the printing time; for a given printing time, the highest values corresponded to the CIT-50 pharma-ink due its higher citrulline content. During printing, extruded CIT-30 exhibited a more liquid consistency, resulting in flatter figures with lower weight (for the same printing time) compared to CIT-50 pharma-ink. The CIT-30 printlets prepared at 60 s showed a less appealing appearance than the rest of the printlets. The formulation was spilled due to the poor consistency of the pharma-ink. Differently, CIT-30 printlets prepared at 30 s and 45 s did not spill over the printing surface and showed a better appearance.

Considering the weight of each printlet and the percentage of citrulline in each pharma-ink, the recoveries were close to 100 %, demonstrating that there was no degradation of citrulline during the printing process and that all the amino acid added was correctly homogenised in the pharma-ink.

A relationship between the printing time (s) and printed dose (mg) as well as printed weight (mg) was established, since at different printing times both printlet parameters varied proportionally. For assessing this last, the doses obtained for CIT-30–60 and CIT-50–60 were taken as a reference, as they were the first printlets prepared. Based on these



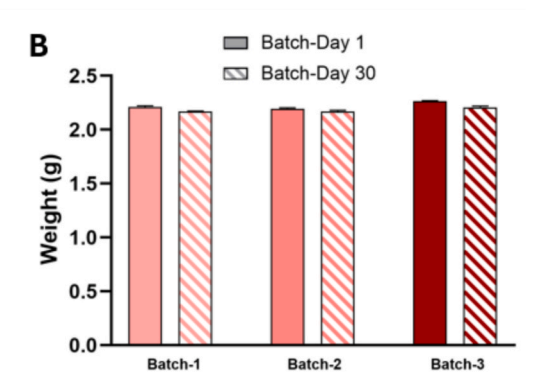
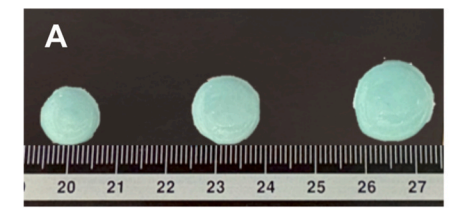


Fig. 6. Graphical representation of the average weight of different batches and their weight after 30 days due to water loss for each formulation: (A) CIT-50 and (B) CIT-30.



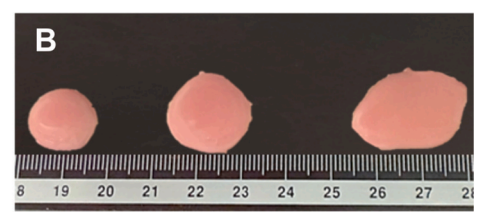


Fig. 8. Image of the produced printlets at different printing times (30 s, 45 s and 60 s) from left to right using: (A) CIT-50 pharma-ink and (B) CIT-30 pharma-ink. The scale bar indicates length in centimeters (cm).

values, theoretical dose and weight values were calculated for both formulations at 30 s and 45 s printing times. Dose accuracy was close to 100 % which enables the prediction of which printing time should be used in order to obtain different doses of citrulline. The CV obtained for the different formulation codes was below 5 %. This indicated a high consistency in the results, demonstrating minimal variability between measurements. Such low CV values confirmed the reliability of the printing process, ensuring uniformity in their performance.

XRPD spectra (Fig. 9A) and DSC scans (Fig. 9B) were used to explore the physical state of each component in the developed pharma-inks and to determine the influence of the different processes until the obtention of the printlets.

The X-ray results (Fig. 9A) exhibited the clearly crystalline structure of the components of the pharma-ink in their pure state. In the case of citrulline, a distinctly pronounced crystallinity peak was observed at 21.54° , as well as at 25.48° and 32.49° (Allouchi et al., 2014). For isomalt, a clear peak appears at 19.96° , along with other peaks of lower intensity from 15 to 28° (Ndindayino et al., 1999). Regarding CIT-30 and CIT-50 pharma-ink bars, the peaks showed less intensity compared to pure isomalt and citrulline. This could be partially attributed to perform the measurement with Göebel optics since the samples were not powder and this caused the peaks to widen.

When comparing pharma-ink pre-printing process CIT-30 and CIT-50, the peaks corresponding to citrulline at 21.54° , 25.48° , and 32.49° were present, with notably higher intensity in CIT-50 pharma-ink than in CIT-30 due to its higher content of citrulline. Isomalt characteristic peaks also appeared near 15° , as well as 19.9° , very close to citrulline

peak. Interestingly, the intensity of these peaks was also higher for CIT-50, despite having a lower percentage of isomalt. Moreover, the intensity of peaks related to both isomalt and citrulline decreased after the post-printing process. Molecules need sufficient mobility to organize into a lattice. When isomalt is mixed with citrulline, the physical processing conditions such as temperature or shear and cooling rate can contribute to changes in crystallinity. Particularly if heated, isomalt might undergo partial amorphization, and at higher concentrations (CIT-30) the amorphous regions tend to increase, while in CIT-50 might undergo less disruption. The balance between isomalt and citrulline in CIT-50 allows for more efficient nucleation and crystal growth. Moreover, during the preparation of pharma-inks citrulline was added at 70 °C while the printing process was carried out at 100 °C, which could lead to a less ordered structure due to kinetic energy.

Moreover, two peaks were observed in the DSC of pure isomalt in Fig. 9B. The first peak (near 100 °C) and the second peak (near 150 °C) were related to its glass transition temperature (T_g) and melting point (T_m), respectively. This melting temperature of pure Isomalt is a common temperature for the vast majority of Isomalt types (Nawatila, 2024; ChemicalBook, 2025). However, for pure citrulline, no peak could be observed. A melting temperature of around 230 °C would be expected since it is in a crystalline state according to XRPD results (Fig. 9A) (PubChem, 2025; Esseku and Adeyeye, 2011). Interestingly, a shift of T_g and T_m from pure isomalt occurred in the pharma-ink and printlet samples for both formulations. T_g exhibited a minor shift with respect to pure isomalt while T_m shifted much more (up to 200 °C). This could be explained by the melting-cooling process during printing and post-

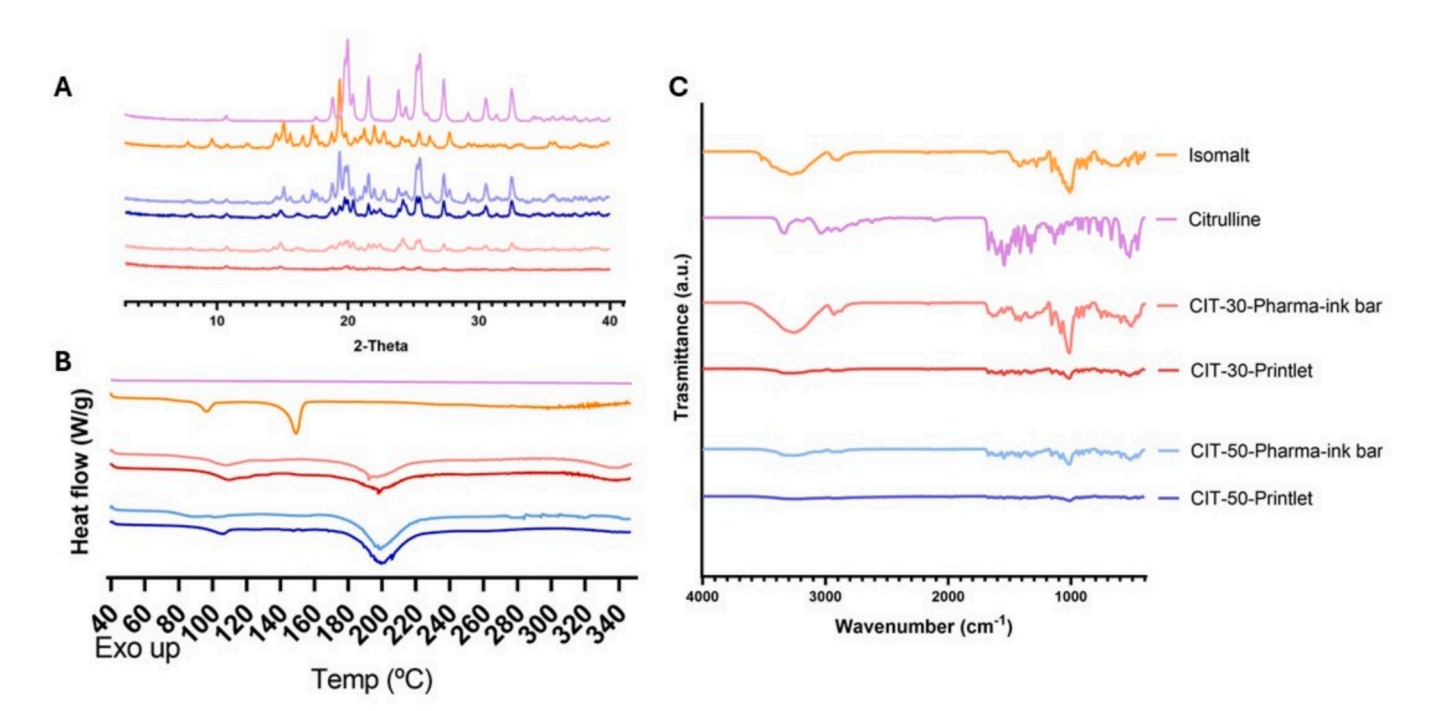


Fig. 9. Results of (A) XRPD, (B) DSC and (C) ATR spectra of isomalt, pure citrulline, pharma-ink bars and printlets. The legend applies to the three plots.

printing.

The ATR spectrum of citrulline δ contained several broad peaks between 3200 and 2400 cm $^{-1}$ related to the ammonium group (Fig. 9C). Also, a peak around 1600 cm $^{-1}$ was attributed to a carboxylate group (Allouchi et al., 2014). This peak was observed in both pharma-inks, and with minimal intensity in the printlets.

3.3. Printlets disintegration and citrulline release

CIT-30–30, CIT-30–60, CIT-50–30 and CIT-50–60 printlets completely disintegrated in less than 15 min, although the time depended on the formulation and printing time (Table 3). CIT-30–30 printlets completely disintegrated in less than 3 min, while CIT-30–60 printlets required 4.38 min. For the CIT-50 formulations, CIT-50–30 exhibited a disintegration time of 6 min, while CIT-50–60 reported a disintegration time of 8 min, being the one that took the longest to disintegrate, yet still well below the 15-minute limit. Thus, it can be concluded that the printlets, regardless of the amount of citrulline (30 % or 50 % w/w) and the printing time (30 s or 60 s), exhibited rapid disintegration.

Moreover, at both printing times of 30 and 60 s, the average disintegration rate (mg/s) was higher for the 30 % w/w formulation, indicating a faster disintegration mainly due to the higher concentration of Isomalt (solubility = 250 g/L) (BENEO, 2025) and, so, lower content of citrulline (solubility = 200 g/L) (PubChem, 2025).

In vitro release profiles for the lowest and highest printing times of each pharma-ink (CIT-30 and CIT-50) are shown in Fig. 10. The printed cylinders eroded in contact with artificial saliva and exhibited an immediate release regardless of the pharma-ink and printing time referred, being completely dissolved in less than 30 min. According to the European Pharmacopoeia (2025b), immediate release dosage form is identified as at least 75 % of the active substance is dissolved within 45 min, while printlets released more than the 80 % of citrulline within the first 12 min of the test. Slightly faster dissolution was observed in CIT-30 comparing with CIT-50 printlets, which can be attributed to differences in the surface-to-volume (SA/V) ratio. For instance, CIT-30–30 printlets had an SA/V ratio of 0.74 \pm 0.02 while for CIT-50–30, it was 0.68 \pm 0.02. This slightly higher SA/V ratio in CIT-30 printlets resulted in a higher surface exposure, facilitating citrulline release.

After 30 days of storage, the pharma-ink bars maintained adequate printability despite water loss. This was evidenced by dose accuracy, which remained close to 100 % (Table 3), indicating consistent ink deposition across all pharma-inks and printing times. These findings support a clear relationship between printing time and pharma-ink deposition required to achieve a specific dose with high accuracy. Moreover, citrulline remained stable within the stored bars, as the recovered amounts were comparable to those from freshly prepared samples. Overall, the results confirm that pharma-ink bars can be stored

Table 3 Disintegration times (n = 3) of printlets produced using fresh CIT-30 and CIT-50 pharma-ink bars; and dose accuracy (%) and recovery (%) (n = 5) of printlets produced using CIT-30 and CIT-50 pharma-ink bars after 30-day storage. Results are expressed as mean \pm SD.

Formulation code	Disintegration time (min)	Average disintegration rate (mg/s)	Dose after 30- day storage (%)	Recovery after 30- day storage (%)
CIT-30-30	$\textbf{2.74} \pm \textbf{0.13}$	4.14 ± 0.20	101.11	100.09 \pm
			± 1.68	1.32
CIT-30-60	4.38 ± 0.16	5.14 ± 0.19	100.98	100.39 \pm
			\pm 2.81	1.26
CIT-50-30	6.01 ± 0.25	1.99 ± 0.08	101.79	99.70 \pm
			\pm 1.56	0.97
CIT-50-60	8.18 ± 0.09	2.94 ± 0.03	100.80	99.61 \pm
			± 1.09	0.89

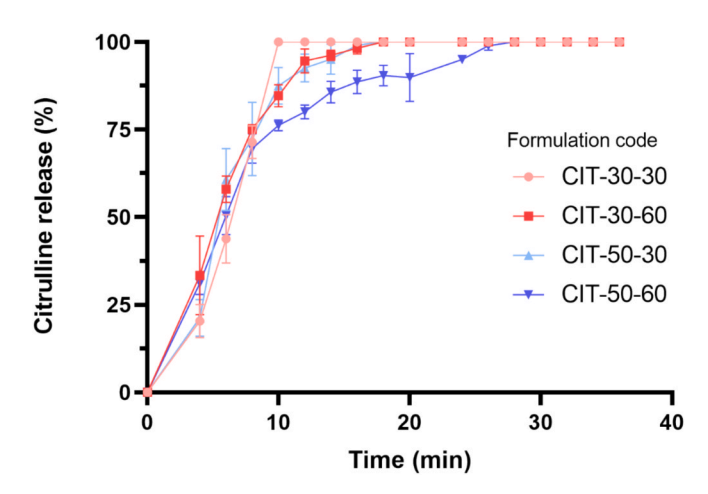


Fig. 10. Citrulline release profiles from CIT-30-30 (pink), CIT-30-60 (red), CIT-50-30 (bright blue) and CIT-50-60 (dark blue) printlets (n=3).

for at least 30 days without compromising printability, amino acid stability, or fracture toughness (Fig. 7). This is particularly important for enabling the advance production and storage of pharma-ink bars for ondemand use in various settings, without affecting process efficiency.

The findings of this study demonstrate the utility of a 3D pen for precise, rapid, and decentralized on-demand drug manufacturing. This portable device successfully extruded pharma-ink bars to produce lozenges containing flexible and accurate doses of citrulline, ranging from 200 to 700 mg. Therapeutic doses usually range between 100 and 200 mg/kg/day, depending on each individual patient according to the international guidelines for OTC Deficiency management (Häberle et al., 2019). The obtained doses were aligned with those reported in recent clinical studies, where chewable printlets of around 600-950 mg of citrulline were printed using SSE for paediatric population affected with OTC Deficiency (Rodríguez-Pombo et al., 2024a). Higher doses can be achieved by increasing the printing time, the citrulline content of the pharma-ink or, even, taking multiple printlets. Notably, the doses achieved in this study were significantly higher than those previously reported for nicotine using a handheld printer (0.60 to 4.30 mg) (Carou-Senra et al., 2025), highlighting the potential of this device for therapies requiring higher dose ranges.

For the development of this study, pharma-ink bars were formulated using only the minimum necessary excipients, distilled water and isomalt. Isomalt serves as a sugar substitute, offering several advantages: it provides a sweet taste without contributing to tooth decay (childfriendly), reduces calorie intake, and is suitable for individuals with conditions like diabetes (Schweitzer et al., 2024). Moreover, isomalt exhibits several advantageous properties, including good chemical, thermal, and microbiological stability (Ndindayino et al., 1999). Although other excipients such as maltitol syrup, glycerin, citric acid, and methyl cellulose were tested—following formulations for lozenges reported in other studies (Kini et al., 2011)—the resulting mixtures were more complex and did not yield satisfactory results, as extrusion was often compromised with intermittent flow. Regarding isomalt, although different types were evaluated, isomalt 960 was selected due to its high hot-extrusion capacity, solubility of 25 g/100 g in water at 20 °C, d50 of 380 µm, and exceptional stability against degradation by temperature, acids, and APIs, as well as its pleasant, sugar-like natural taste (BENEO, 2025). No organic solvents were involved and the formulation process also allowed for the incorporation of colourants and flavouring agents, enhancing the organoleptic properties, ultimately improving patient acceptance. Moreover, the extrusion of developed pharma-ink bars took the form of lozenges, closely resembling hard candies. Unlike tablets or capsules that need to be swallowed, lozenges are meant to be dissolved in the mouth, which is particularly beneficial for paediatrics, the elderly, and patients with swallowing difficulties (Kulkarni et al., 2022). In this

regard, they demonstrated a disintegration time ranging from 2 to 8 min, depending on the weight of the printlet and pharma-ink used. It is important to note that the disintegration and dissolution tests used in these evaluations, while informative, do not fully replicate the conditions within the oral cavity, where suction and other physiological factors may further accelerate the disintegration and dissolution processes. Consequently, the in vivo disintegration and dissolution times may be even shorter than the results obtained in vitro. These findings aligned with previously reported data on lozenges, which typically disintegrate within 6 to 8 min (Raina et al., 2023; Halagali et al., 2022). Additionally, lozenges could be developed for both systemic treatments and localized therapies (Kotlyar et al., 2020; Dudek et al., 2023), making them a highly versatile pharmaceutical option even for veterinary.

Although this proof-of-concept study was conducted under controlled laboratory conditions, the promising results suggest that such portable systems could play a crucial role in enabling on-demand drug production in resource-limited or remote settings, where space and energy are constrained. Potential future applications include deployment in remote areas, mobile medical units, and even in-home therapeutic preparation. This aligns with the broader goal of healthcare decentralization, which aims to improve access to personalized medicine (Chan and Ginsburg, 2011). Moreover, the 30-day stability of the pharma-ink bars was demonstrated, with both printability and dose accuracy maintained over time. This indicates that the bars produced can be used on demand or stored for later use, enabling the preparation of the required number of dosage forms when needed in decentralized environments. Although the mentioned stability studies showed that no degradation occurred at 20 °C after 30 days, it would also be interesting to evaluate their stability under the environmental conditions defined for different climatic zones (I-IV) in future studies, considering that the handheld 3D pen could potentially be employed in diverse geographical settings. Stability studies would be carried out following section 7.2 Considerations for Products Intended to be Stored at Room Temperature of the ICH Q1 guideline, taking into account both the climatic zone and the type of study (long-term, intermediate, and accelerated) (EMA, 2025).

To enable the implementation of this device in decentralized medicine production, following the evolution of desktop 3D printers, specialized portable pharmaceutical printing devices should be developed to meet regulatory standards. Among potential improvements, incorporating a disposable internal structure could enhance device safety by reducing the risk of cross-contamination and eliminating the need for high-temperature cleaning processes, thereby simplifying maintenance and ensuring a hygienic operating environment. Similar to the concept of SSE printheads, such a design would allow complete isolation of the formulation from other parts of the pen. This would further strengthen safety and provide better control over the formulation during the printing process. Further studies will require to evaluate the safety of operators using the device to avoid health issues to the user (Stefaniak et al., 2025).

Additionally, several features could be added to the portable device to provide greater control over the printing process. A more sophisticated plunger could allow for a more controlled material flow and apply higher force (N), facilitating the printing of pharma-inks with more resistant rheological properties. A precise temperature control inner system would not only maintain a constant temperature regardless of location but also allow adjustment to the optimal extrusion temperature for different pharma-ink bars. Finally, an internal timer could regulate printing times accurately, initiating and stopping the extrusion automatically. These improvements would support the deployment of such devices across diverse environments.

It is important to highlight that 3D printing technologies are primarily intended for the production of small batches of medicines, where the application of conventional quality control systems would be largely destructive. For this reason, new evaluation strategies have been proposed. For example, the use of near-infrared spectroscopy (NIR) enables non-destructive determination of drug content (Jørgensen et al., 2025),

offering a feasible option for in-process control across different environments. In addition, since a correlation between printing time, weight, and dose was established, the availability of a balance could allow straightforward monitoring of the printing process in decentralized settings. Incorporating a pressure sensor in the plunger would also provide valuable information, as maintaining a continuous flow is essential to achieve a consistent deposition of the ink. Indeed, similar sensors have already been integrated into SSE printheads of desktop printers to monitor flow, supporting the feasibility of this approach (Díaz-Torres et al., 2022). Altogether, these approaches would improve quality control in diverse environments, complemented by the periodic random selection of printed samples for HPLC analysis to confirm the established time—weight—dose relationship.

4. Conclusions

For the first time, a 3D portable pen was successfully used to produce personalized medicines containing precise and flexible doses of citrulline for the treatment of OTC, a rare disease affecting paediatric patients. Pharma-ink bars containing different percentages of amino acid (30 % and 50 % w/w) and varying colourants and flavouring agents were manufactured with similar dimensions to the commercial bars. Only eco-friendly excipients were used being Isomalt, a sugar substitute, the main component, along with distilled water; while no organic-solvents were involved. Pharma-ink bars were used to produce lozenges with tailored citrulline doses modifying printed area and printing time. Printing by area was discarded early due to the high intra- and interindividual variability caused by differences in printing pattern and speed; following different directions or printing faster or slower led to large variations in ink deposition. By contrast, varying the printing time enabled a precise and reliable correlation with the final dosage. The resulting printlets obtained at different printing times exhibited personalized dosing, with dose accuracy and recovery near 100 %. Moreover, an 80 % of the amino acid was released within the first 12 min of testing. Additionally, pharma-ink bars storage during a 30-day period showed a minimum water loss (\sim 2%) and maintained their printability, exhibiting dose accuracy and recoveries similar of those obtained with freshly pharma-ink bars, with no citrulline degradation. This finding evidences their stability and suitability for prolonged storage, ensuring on-demand printing without compromising product quality.

Above all, this study proposed and implemented the use of 3D pens as a viable option to bring on-demand personalized drug production to areas where larger systems are impractical. The portability exhibited by these devices, along with their energy and space efficiency, makes them a cost-effective and resource-efficiency optimized alternative for limited areas. Following the path paved by specialized desktop 3D printers, the future development of portable printing devices- capable of meeting regulatory standards- could make personalized medicine accessible to all sectors in population.

Funding sources

This work was funded by Fundación Mutua Madrileña (XIX Edition of Fundación Mutua Madrileña Research Grants [AP180872022]) and partially funded by Spain Ministerio de Ciencia e Innovación MCIN/AEI/https://doi.org/10.13039/501100011033 [PID2023-149544OB-C22], Xunta de Galicia [ED431C 2024/09] and FEDER.

CRediT authorship contribution statement

Paola Carou-Senra: Writing – review & editing, Writing – original draft, Visualization, Validation, Software, Methodology, Investigation, Formal analysis, Data curation, Conceptualization. Lucía Rodríguez-Pombo: Writing – review & editing, Writing – original draft, Visualization, Validation, Methodology, Investigation, Data curation, Conceptualization. Laura Castro-Martínez: Writing – original draft,

Visualization, Validation, Methodology, Investigation, Conceptualization. Abdul W. Basit: Writing - review & editing, Supervision, Resources, Project administration, Funding acquisition, Conceptualization. Carmen Alvarez-Lorenzo: Writing - review & editing, Writing - original draft, Supervision, Resources, Project administration, Methodology, Funding acquisition, Formal analysis, Conceptualization. Alvaro Goyanes: Writing - review & editing, Supervision, Resources, Project administration, Methodology, Funding acquisition, Formal analysis, Conceptualization.

Declaration of competing interest

The authors declare the following financial interests/personal relationships which may be considered as potential competing interests: Alvaro Govanes reports equipment, drugs, or supplies was provided by Spain Ministry of Science and Innovation. Carmen Alvarez-Lorenzo reports financial support was provided by Government of Galicia Department of Education Science Universities and Professional Training. Alvaro Goyanes reports financial support was provided by Mutua Madrileña Foundation. Alvaro Goyanes reports a relationship with FABRX Ltd that includes: equity or stocks. Abdul W Basit reports a relationship with FABRX Ltd that includes: equity or stocks. Carmen Alvarez-Lorenzo and Abdul W. Basit are Editors of the International Journal of Pharmaceutics. Given their role as Editors, they had no involvement in the peer review of this article and had no access to information regarding its peer review. Full responsibility for the editorial process for this article was delegated to another journal editor. If there are other authors, they declare that they have no known competing financial interests or personal relationships that could have appeared to influence the work reported in this paper.

Acknowledgments

PCS acknowledges a predoctoral fellowship [Programa de axudas á etapa predoutoral, grant number ED481A 2023] from Xunta de Galicia (Consellería de Cultura, Educación, Formación Profesional e Universidades). LRP acknowledges the predoctoral fellowship [FPU20/ 01245] provided by the Ministerio de Universidades [Formación de Profesorado Universitario (FPU 2020)].

Data availability

Data will be made available on request.

References

- Allouchi, H., Nicolaï, B.A., Barrio, M., Céolin, R., Mahé, N., Tamarit, J.-L., Do, B., Rietveld, I.B., 2014. On the polymorphism of l-citrulline: crystal structure and characterization of the orthorhombic δ form. Cryst. Growth Des. 14, 1279-1286. https://doi.org/10.1021/cg401801u.
- BENEO, Excipientes farmacéuticos Productos farmacéuticos. https://www.beneo.com/ es/excipientes-farmaceuticos/productos-farmaceuticos, 2025.
- Carou-Senra, P., Awad, A., Basit, A.W., Alvarez-Lorenzo, C., Goyanes, A., 2025. Harnessing handheld inkjet printing technology for rapid and decentralised fabrication of drug-loaded hydroxypropyl cellulose buccal films. Carbohydr. Polym. Technol. Appl. 9, 100724. https://doi.org/10.1016/j.carpta.2025.100724.
- Chan, I.S., Ginsburg, G.S., 2011. Personalized medicine: progress and promise. Annu. Rev. Genomics Hum. Genet. 12, 217–244. https://doi.org/10.1146/annurev-genom-082410-101446
- ChemicalBook. Isomalt [Internet]. Access Date: May 13th, 2025. Available from: https:// www.chemicalbook.com/ChemicalProductProperty_EN_CB1309643.htm.
- Cui, M., Pan, H., Fang, D., Qiao, S., Wang, S., Pan, W., 2020. Fabrication of high drug loading levetiracetam tablets using semi-solid extrusion 3D printing. J. Drug Deliv. Sci. Technol. 57, 101683, https://doi.org/10.1016/j.iddst.2020.101683
- Díaz-Torres, E., Rodríguez-Pombo, L., Ong, J.J., Basit, A.W., Santoveña-Estévez, A., Fariña, J.B., Alvarez-Lorenzo, C., Goyanes, A., 2022. Integrating pressure sensor control into semi-solid extrusion 3D printing to optimize medicine manufacturing. Int. J. Pharm.: X 4, 100133. https://doi.org/10.1016/j.ijpx.2022.100133.
- Dudek, B., Tymińska, J., Szymczyk-Ziółkowska, P., Chodaczek, G., Migdał, P., Czajkowska, J., Junka, A., 2023. In vitro activity of octenidine dihydrochloridecontaining lozenges against biofilm-forming pathogens of oral cavity and throat. Appl. Sci. 13, 2974. https://doi.org/10.3390/app13052974.

- Ehtezazi, T., Algellay, M., Islam, Y., Roberts, M., Dempster, N.M., Sarker, S.D., 2018. The application of 3D printing in the formulation of multilayered fast dissolving oral films. J. Pharm. Sci. 107, 1076-1085. https://doi.org/10.1016/j.xphs.2017.1
- EMA. ICH Q1 Guideline on stability testing of drug substances and drug products 2025 [cited 2025 Aug 18]; Available from: https://www.ema.europa.eu/en/ich-q1guideline-stability-testing-drug-substances-drug-products.
- Esseku, F., Adeyeye, M.C., 2011. Bacteria and pH-sensitive polysaccharide-polymer films for colon targeted delivery. Crit. Rev. Ther. Drug Carrier Systs. 28, 395-445. https:// doi.org/10.1615/CritRevTherDrugCarrierSyst.v28.i5.10.
 European Pharmacopoeia, 12th edition. 2.9.1. Disintegration of tablets and capsules.
- Council of Europe, Strasbourg, France, 2025a.
- European Pharmacopoeia, 12th edition. 5.17.1. Recommendations on dissolution testing. Council of Europe, Strasbourg, France, 2025b.
- Genina, N., Fors, D., Palo, M., Peltonen, J., Sandler, N., 2013. Behavior of printable formulations of loperamide and caffeine on different substrates-Effect of print density in inkjet printing. Int. J. Pharm. 453, 488-497. https://doi.org/10.1016/j.
- Häberle, J., Burlina, A., Chakrapani, A., Dixon, M., Karall, D., Lindner, M., Mandel, H., Martinelli, D., Pintos-Morell, G., Santer, R., 2019. Suggested guidelines for the diagnosis and management of urea cycle disorders: first revision. J. Inherit. Metab. Dis. 42, 1192-1230. https://doi.org/10.1002/jimd.12100.
- Halagali, P., Bolmal, U.B., Patil, A.S., 2022. Development and evaluation of paracetamol lozenges, World. J. Pharm. Res. 11, 1326-1330. https://doi.org/10.20959
- Ianno, V., Vurpillot, S., Prillieux, S., Espeau, P., 2024. Pediatric formulations developed by extrusion-based 3D printing: from past discoveries to future prospects. Pharmaceutics. 16, 441. https://doi.org/10.3390/pharmaceutic
- Januskaite, P., Goyanes, A., Orlu, M., Basit, A.W., 2025. Inkjet printing of pharmaceutical tattoos for the direct deposition of oestradiol onto skin in turner syndrome. Eur. J. Pharm. Biopharm. 214, 114798. https://doi.org/10.1016/j.
- Jørgensen, A.K., Dowek, A., Denis, L., Ong, J.J., Annereau, M., Rieutord, A., Parhizkar, M., Goyanes, A., Basit, A.W., 2025. 3D printing personalized medications in a hospital: Rapid and non-destructive dose verification of printed medicines enabled by miniaturised spectroscopy. J. Pharm. Sci. 114 (9), 103895. https://doi. org/10.1016/j.xphs.2025.103895.
- Karavasili, C., Gkaragkounis, A., Moschakis, T., Ritzoulis, C., Fatouros, D.G., 2020. Pediatric-friendly chocolate-based dosage forms for the oral administration of both hydrophilic and lipophilic drugs fabricated with extrusion-based 3D printing. Eur. J. Pharm. Sci. 147 (2020), 105291. https://doi.org/10.1016/j.ejps.2020.105291
- Khaled, S.A., Burley, J.C., Alexander, M.R., Yang, J., Roberts, C.J., 2015. 3D printing of five-in-one dose combination polypill with defined immediate and sustained release profiles, J Control Release 217, 308-314, https://doi.org/10.1016/j. iconrel, 2015, 09, 028.
- Kini, R., Rathnanand, M., Kamath, D., 2011. Investigating the suitability of Isomalt and liquid glucose as sugar substitute in the formulation of Salbutamol sulfate hard candy lozenges. J Chem Pharm Res. 3 (4), 69-75.
- Kotlyar, M., Vogel, R.I., Dufresne, S.R., Mills, A.M., Vuchetich, J.P., 2020. Effect of nicotine lozenge use prior to smoking cue presentation on craving and withdrawal symptom severity. Drug Alcohol Depend. 206, 107706. https://doi.org/10.1016/j. drugalcdep.2019.107706.
- Kulkarni, M.P., Sharma, A., Tanwar, S., Vandana, P.B., Wadhwa, S., Singh, G., Kumar, P., Kumar, R., 2022. Pharmaceutical lozenges: recent trends and developments with an update on research and patents. Recent Adv. Drug Deliv. Formul. 16, 45–54. https:// doi.org/10.2174/2667387816666211231103759
- Kumari, J., Pandey, S., Jangde, K.K., Kumar, P.V., Mishra, D.K., 2024. Evolution, integration, and challenges of 3D printing in pharmaceutical applications: a comprehensive review. Bioprinting. 44, e00367. https://doi.org/10.1016/j. bprint.2024.e00367
- Liu, L., Fu, K., Hong, S., Wang, Z., Mo, M., Li, S., Yu, Y., Chen, J., Chen, J., Zeng, W., 2023. Improving the quality and clinical efficacy of subdivided levothyroxine sodium tablets by 3D printing technology. J. Drug Deliv. Sci. Tech. 89, 105008. https://doi.org/10.1016/j.jddst.2023.105008.
- Lyousoufi, M., Lafeber, I., Kweekel, D., de Winter, B.C.M., Swen, J.J., Le Brun, P.P.H., Bijleveld-Olierook, E.C.M., van Gelder, T., Guchelaar, H.J., Moes, D.J.A.R., 2023. Development and bioequivalence of 3D-printed medication at the point-of-care: bridging the gap toward personalized medicine. Clin. Pharmacol. The. 113, 1125-1131. https://doi.org/10.1002/cpt.2870.
- Milliken, R.L., Quinten, T., Andersen, S.K., Lamprou, D.A., 2024. Int. J. Pharm. 653, 123902. https://doi.org/10.1016/j.jconrel.2015.09.028
- Nawatila R., Formulation and physical characteristic of hard candy lozenge of citrus limon essential oil on various types of sugar free candy base (Isomalt, Mannitol, Sorbitol), Pharm. J. Indones. 10 (2024) 53-58. 10.21776/ub.pji.2024.010.01.8.
- Ndindayino, F., Henrist, D., Kiekens, F., Vervaet, C., Remon, J.P., 1999. Characterization and evaluation of isomalt performance in direct compression. Int. J. Pharm. 189, 113-124. https://doi.org/10.1016/S0378-5173(99)00241-0.
- PubChem. Compound Summary for CID 9750, Citrulline [Internet]. Access Date: May 13th, 2025. Available from: https://pubchem.ncbi.nlm.nih.gov/compound/2S_-2amino-5-_carbamoylamino_pentanoic-acid.
- Raina D., M. Kumar, B. Rana, P. Mall, Formulation and evaluation of Chocolate Lozenges for cessation of smoking, UJPAH 34 (2023) 1-7. 10.51129/ujpah-2022-34-1(9).
- Rodríguez-Pombo, L., Gallego-Fernández, C., Jørgensen, A.K., Parramon-Teixidó, C.J., Cañete-Ramirez, C., Cabañas-Poy, M.J., Basit, A.W., Alvarez-Lorenzo, C., Goyanes, A., 2024a. 3D printed personalized therapies for pediatric patients affected by adrenal insufficiency. Expert Opin. Drug Deliv. 21, 1665-1681. https://doi.org/

- Rodríguez-Pombo, L., de Castro-López, M.J., Sánchez-Pintos, P., Giraldez-Montero, J.M., Januskaite, P., Duran-Piñeiro, G., Bóveda, M.D., Alvarez-Lorenzo, C., Basit, A.W., Goyanes, A., 2024b. Paediatric clinical study of 3D printed personalised medicines for rare metabolic disorders. Int. J. Pharm. 657, 124140. https://doi.org/10.1016/j. ijpharm.2024.124140.
- Schweitzer, L., Wouters, R., Theis, S., 2024. Replacing sugar with the polyol isomalt: technological advances and nutritional benefits focusing on blood glucose management. Nutrafoods. 551–559. https://doi.org/10.17470/NF-024-0064.
- Seoane-Viaño, I., Januskaite, P., Alvarez-Lorenzo, C., Basit, A.W., Goyanes, A., 2021. Semi-solid extrusion 3D printing in drug delivery and biomedicine: personalised solutions for healthcare challenges. J. Control Release. 332, 367–389. https://doi. org/10.1016/j.jconrel.2021.02.027.
- Sjöholm, E., Sandler, N., 2019. Additive manufacturing of personalized orodispersible warfarin films. Int. J. Pharm. 564, 117–123. https://doi.org/10.1016/j.ijpharm.2019.04.018.
- Stefaniak, A.B., Bowers, L.N., Brusak, E.D., Streicher, R.P., Goyanes, A., Friend, S.A., Hammond, D.R., LeBouf, R.F., Qi, C., M., 2025. Abbas Virji, Influence of filament loading technique on surrogate active pharmaceutical ingredient particle emissions during material extrusion 3D printing of tablets. Int. J. Pharm. 682, 125980. https://doi.org/10.1016/j.ijpharm.2025.125980.
- Tong, H.X., Zhang, J.H., Ma, J., Zhang, J.M., 2024. Perspectives on 3D printed personalized medicines for pediatrics. Int. J. Pharm. 653, 123867. https://doi.org/ 10.1016/j.ijpharm.2024.123867.